PERGAMON

International Journal of Solids and Structures 37 (2000) 563–576

INTERNATIONAL JOURNAL OF SOLIDS and STRUCTURES

www.elsevier.com/locate/ijsolstr

Magnetoelastic analysis of non-circular superconducting partial torus

Xiao Jing Zheng*, Xingzhe Wang, You-He Zhou

Department of Mechanics, Lanzhou University, Lanzhou, 730000, P. R. China

Received 26 February 1998; in revised form 12 November 1998

Abstract

In this paper, we present a theoretical analysis of magnetoelasticity for a set of superconducting partial torus with D-typed non-circular coils. This kind of coil is an essential model adopted in the new conception design of Tokamak fusion reactors. Its magneto–mechanical behavior, including bending and snapping, is simulated with the aid of the curved beam theory and the Biot–Savart law. A semi-analytical method is employed to quantitatively solve the boundary-value equations of the coil. The effects of the radius ratio $\lambda = R_1/R_2$ of the coil on the critical snapping current, the deformation and the internal force components of the coil are discussed. It is found that the critical current increases and the deformation decreases with the increase of the ratio $\lambda = R_1/R_2$, and small misalignments of the coils make the critical current lower.

Keywords: Non-circular D-typed coil; Superconducting partial torus; Bending and instability; Magnetoelasticity; Critical current; Effect of radius ratio

1. Introduction

With the rapid increase in the consumption of energy, it is important to find new energy resources. Development of nuclear fusion as a practical energy source would provide great benefits. In the conception, design and construction of an experimental fusion reactor, high magnetic fields are created by superconducting coils to keep the plasma from cooling off on the reactor vessel walls. The coil is subjected to magnetic forces produced by the interaction of the coil with magnetic fields from nearby coils. Magnetoelastic bending and snapping of the coil have been

* Corresponding author. Tel.: +0086-931-8911727; Fax: +0086-931-8625576.
E-mail address: zhouyh@lzu.edu.cn (X.J. Zheng)

0020-7683/00/$ - see front matter
PII: S0020-7683(99)00018-9

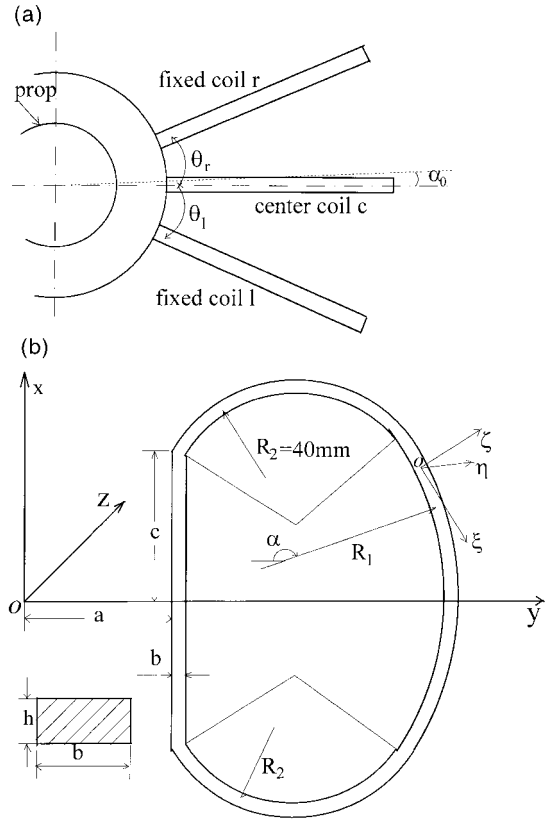

Fig. 1. Non-circular three-coil partial torus: (a) top view, (b) side view and coordinate systems.

observed experimentally. Since structural devices are often load limited by the bending and snapping of the structural elements, it is necessary to quantitatively analyze the mechanical behavior of the coil for the safety of the reactor.

Moon (1976) and Moon and Swanson (1977) were the first to conduct an experiment and gave an analytical model for magnetoelastic snapping of superconducting coils. In his theoretical prediction, the critical current was obtained when the frequency of the out-of-plane vibration of a current-carrying coil becomes zero. Geiger and Jungst (1991) used this method to investigate the TESPE toroidal magnet system. Miya et al. (1980) and Miya and Uesaka (1982) adopted the finite element method to obtain the theoretical prediction for the critical current; they also performed an experiment of a three-coil superconducting partial torus. Aside from the investigation on the snapping of the coil, Motojima (1993) simulated the magnetoelastic bending of the coil by an uncoupled theoretical model. It should be noted that only one kind of mechanical behavior, either bending or snapping, can be simulated by the above methods. A nonlinear mathematical model (Zhou et al., 1995) was recently presented for describing the magnetoelastic behavior, both bending and snapping, of D-typed circular coils in a partial torus. Their theoretical prediction for the critical current is in a good agreement with Miya's experimental data (Miya and Uesaka, 1982). However, all these researches only focus on the circular coil. Since more and more coils installed in a superconducting Tokamak are non-circular ones which have not been investigated in the literature, we should pay more attention to the non-circular coils.

In this paper, we will analyze the magnetoelastic bending and snapping of a superconducting non-circular coil composed of several circular arcs with different radii. A theoretical model is suggested for the non-circular coil based on the curved beam theory and the Biot–Savart law. The effect of the elastic deformation, including in-plane and out-of-plane bending, axial extension and torsion, of the coil on the critical current is considered. A semi-analytical and semi-numerical solution combined by an exact fundamental solution to the homogeneous differential equations and a numerical particular solution to the inhomogeneous differential equations is obtained for the nonlinear boundary-value equations of the problem. For the non-circular coil composed of three circular arcs with different radii, the effect of the radius ratio, $\lambda = R_1/R_2$, on the magneto–mechanical behavior is discussed in detail. The numerical results show that there may exist an optimum value for the ratio $\lambda = R_1/R_2$, e.g., 1.382, for which the critical current is higher and the internal forces are lower than those for the other values. Moreover, the numerical results confirm that small misalignments of coils will influence the critical snapping current. These results are useful to the study and design of a fusion reactor with non-circular D-typed superconducting coils.

2. Basic equations

In a three-coil superconducting partial tours, the current-carrying coils are non-circular and D-typed. A deformable coil, called coil c, is symmetrically placed between two fixed side coils, respectively called coil l and coil r, see Fig. 1. To examine the bending and the snapping of coil c, we first establish a fixed global coordinate system $Oxyz$ and a local coordinate system $o\xi\eta\zeta$ whose unit vectors are $\mathbf{e}_1$ (along the tangent direction of the axis of the coil c), $\mathbf{e}_3$ (along the normal to the axis of the coil c and lies in the plane of the coil c) and $\mathbf{e}_2$ ($=\mathbf{e}_3 \times \mathbf{e}_1$) (normal to the plane of the coil c), respectively. Then the effect of the deformation of the coil c on its equlibrium configuration is neglected since only the small elastic deformation is considered here. Finally, the basic equation combines equilibrium equations with elastic equations for the deformed coil c in the local coordinate system $o\xi\eta\zeta$ can be written as follows (Love, 1944):

$$\left(\frac{\mathrm{d}N_1}{\mathrm{d}\xi} + \chi_{13}Q_3 + q_1\right)\mathbf{e}_1 + \left(\frac{\mathrm{d}Q_2}{\mathrm{d}\xi} - \chi_{23}Q_3 + q_2\right)\mathbf{e}_2 + \left(\frac{\mathrm{d}Q_3}{\mathrm{d}\xi} - \chi_{13}N_1 + \chi_{23}Q_2 + q_3\right)\mathbf{e}_3 = \mathbf{0}, \tag{1}$$

$$\begin{aligned}&\left(\frac{\mathrm{d}M_1}{\mathrm{d}\xi} + \chi_{13}M_3 + m_1\right)\mathbf{e}_1 + \left(\frac{\mathrm{d}M_2}{\mathrm{d}\xi} - \chi_{23}M_3 - Q_3 + m_2\right)\mathbf{e}_2 \\ &\quad + \left(\frac{\mathrm{d}M_3}{\mathrm{d}\xi} - \chi_{13}M_1 + \chi_{23}M_2 + Q_2 + m_3\right)\mathbf{e}_3 = \mathbf{0},\end{aligned} \tag{2}$$

$$\frac{N_1}{EF} = \frac{\mathrm{d}u}{\mathrm{d}\xi} + \chi_{13}w, \tag{3}$$

$$\frac{M_3}{EJ_3} = \frac{\mathrm{d}^2 v}{\mathrm{d}\xi^2} - \frac{\mathrm{d}}{\mathrm{d}\xi}(\chi_{23}w) - \chi_{23}\left(\frac{\mathrm{d}w}{\mathrm{d}\xi} - \chi_{13}u + \chi_{23}v\right) - \phi\chi_{13}, \tag{4}$$

$$\frac{M_2}{EJ_2} = -\frac{\mathrm{d}^2 w}{\mathrm{d}\xi^2} + \frac{\mathrm{d}}{\mathrm{d}\xi}(\chi_{13}u) - \frac{\mathrm{d}}{\mathrm{d}\xi}(\chi_{23}v) - \chi_{23}\left(\frac{\mathrm{d}v}{\mathrm{d}\xi} - \chi_{23}w\right) + \chi_{13}\left(\frac{\mathrm{d}u}{\mathrm{d}\xi} + \chi_{13}w\right) \tag{5}$$

$$\frac{M_1}{K} = \frac{\mathrm{d}\phi}{\mathrm{d}\xi} + \chi_{13}\left(\frac{\mathrm{d}v}{\mathrm{d}\xi} - \chi_{23}w\right), \tag{6}$$

in which $\chi_{13} = -\mathbf{e}_3 \cdot \frac{\mathrm{d}\mathbf{e}_1}{\mathrm{d}\xi}$ and $\chi_{23} = \mathbf{e}_3 \cdot \frac{\mathrm{d}\mathbf{e}_2}{\mathrm{d}\xi}$ are curvatures of the coil c before it deformed; $\mathbf{P}(\xi) = N_1(\xi)\mathbf{e}_1 + Q_2(\xi)\mathbf{e}_2 + Q_3(\xi)\mathbf{e}_3$ and $\mathbf{M}(\xi) = M_1(\xi)\mathbf{e}_1 + M_2(\xi)\mathbf{e}_2 + M_3(\xi)\mathbf{e}_3$ are the internal force vector and the internal moment vector of the coil c, respectively; F is the cross section of the coil; J_2 and J_3 are the inertial moments of the section about the η- and ζ-axes, respectively; $\mathbf{U}(\xi) = u\mathbf{e}_1 + v\mathbf{e}_2 + w\mathbf{e}_3$ is the displacement vector of the coil c; ϕ is the torsional angle; $\mathbf{q} = q_1\mathbf{e}_1 + q_2\mathbf{e}_2 + q_3\mathbf{e}_3$ and $\mathbf{m} = m_1\mathbf{e}_1 + m_2\mathbf{e}_2 + m_3\mathbf{e}_3$ are a magnetic force vector and a moment vector exerted on the centerline of the coil c, respectively. According to the Biot–Savart law and the Lorentz law, and neglecting the effect of the self-field on both the magnetic force and on the magnetic moment (Moon, 1984), we have (see Zhou et al., 1995) $\mathbf{m}(\mathbf{r}_c) = \mathbf{0}$ and

$$\mathbf{q}(\mathbf{r}_c) = q_1\mathbf{e}_1 + q_2\mathbf{e}_2 + q_3\mathbf{e}_3 = \frac{\mu I_l I_c}{4\pi}\int_{S_l} \mathbf{e}_1 \times \left[\frac{d\mathbf{r}_l \times \mathbf{r}_l^c}{\left(r_l^c\right)^3}\right] + \frac{\mu I_r I_c}{4\pi}\int_{S_r} \mathbf{e}_1 \times \left[\frac{\mathrm{d}\mathbf{r}_r \times \mathbf{r}_r^c}{\left(r_r^c\right)^3}\right], \tag{7}$$

where μ is the permeability in a vacuum; $\mathbf{r}_l$, $\mathbf{r}_r$ and $\mathbf{r}_c$ are the position vectors of the coil l, the coil r and the coil c, respectively, which are usually expressed as a function on the variable ξ; $\mathbf{r}_l^c$ or $\mathbf{r}_r^c$ are the relative position vector between the centerline of the coil l or the coil r and the centerline of the deformed coil c, that is

$$\mathbf{r}_l^c = \mathbf{r}_c + \mathbf{U}(\xi) - \mathbf{r}_l$$

$$\mathbf{r}_r^c = \mathbf{r}_c + \mathbf{U}(\xi) - \mathbf{r}_r. \tag{8}$$

It should be noted that Eq. (7) is obtained based on some assumptions:

1. the coil is isotropic and homogeneous with equivalent elastic modulus,
2. the distribution of the current is uniform across the cross-section of the coil,
3. the distribution of magnetic field in the coil can be treated as that of a normal conductor, and
4. the cross sectional dimension of the coil is much smaller than the distance between two adjacent coils.

Although superconducting currents flow only on or near the surface of superconducting filaments, assumptions (2) and (3) may be reasonable since the coil is made of multi-filaments which are more or less evenly distributed.

From Eq. (8), one can find that the magnetic force $\mathbf{q}(\mathbf{r}_c)$ and the displacement $\mathbf{U}(\xi)$ of the coil c are mutually coupled. In other words, the magnetic force can affect the deformation of the coil c and, conversely, the deformation of the coil c causes a change in the magnetic force. This kind of interaction makes the basic equations (Eqs. (1)–(6)) nonlinear.

Usually, the carrying current coils in a superconducting torus have the same geometrical sizes and are symmetrically placed in the toroidal direction. For this case, we have $I_l = I_c = I_r = I$, $\theta_l = \theta_r$. For an arbitrary pair of symmetry points on coil l and coil r, respectively, when $v(\xi) \equiv 0$, we have

$$\left(r_l^c\right)_1 = \left(r_r^c\right)_1, \quad \left(r_l^c\right)_2 = -\left(r_r^c\right)_2, \quad \left(r_l^c\right)_3 = \left(r_r^c\right)_3 \tag{9}$$

$$\mathrm{d}(r_l)_1 = \mathrm{d}(r_r)_1, \quad \mathrm{d}(r_l)_2 = -\mathrm{d}(r_r)_2, \quad \mathrm{d}(r_l)_3 = \mathrm{d}(r_r)_3 \tag{10}$$

and $r_l^c = r_r^c$. Therefore, Eq. (7) is then

$$\mathbf{q}(\mathbf{r}_c) = \frac{\mu I^2}{4\pi}\int_{S_l} \mathbf{e}_1 \times \left[\frac{\mathrm{d}\mathbf{r}_l \times \mathbf{r}_l^c}{\left(r_l^c\right)^3} + \frac{\mathrm{d}\mathbf{r}_r \times \mathbf{r}_r^c}{\left(r_r^c\right)^3}\right] = \frac{\mu I^2}{4\pi}\int_{s_l} \frac{2}{\left(r_l^c\right)^3}\left[\left(r_l^c\right)_3 \mathrm{d}(r_l)_1 - \left(r_l^c\right)_1 \mathrm{d}(r_l)_3\right]\mathbf{e}_3, \tag{11}$$

which shows that $\mathbf{q}(\mathbf{r}_c)\cdot\mathbf{e}_2 = 0$. That is, there is no transverse magnetic force component on the coil c when the side coils are symmetrically placed and $v(\xi) \equiv 0$. This means that a trivial solution of the out-of-plane deflection is always the solution to the problem. Since the governing equations are nonlinear, it is possible that there exists a nontrivial solution of the out-of-plane transverse bending deformation when the applied current approaches a critical value. This phenomenon is referred to as magnetoelastic snapping (buckling). However, in practice, it is unavoidable that there exist some misalignments described by an initial small angle α_0 (see Fig. 1) to the symmetry of the coils, which usually leads to $\mathbf{q}(\mathbf{r}_c)\cdot\mathbf{e}_2 \neq 0$. For this case, there exists the out-of-plane deformation of the coil c, referred to as magnetoelastic bending. As the applied current increases, the deformation increases nonlinearly until the coil loses stability. Here, we shall pay more attention to searching the critical snapping current and discussing the effect of misalignments on the critical snapping current.

3. Solving programe

In general, it is not easy to get a set of analytical solutions to Eqs. (1)–(6) since these differential equations are nonlinear ones with variable coefficients. Here, we will use a semi-analytical and semi-numerical method to obtain the solution to Eqs. (1)–(6). Dividing the region of the non-circular coil c into N circular arcs with different radii R_i (i = 1,2,..., N), for each circular arc, we can simplify Eqs. (1)–(6) as follows:

$$\frac{\mathrm{d}\mathbf{Y}_i(\xi)}{\mathrm{d}\xi} = \mathbf{A}_i\mathbf{Y}_i(\xi) + \mathbf{F}_i(\xi), \tag{12}$$

in which $\mathbf{F}_i(\xi) = [-q_1, -q_2, -q_3, 0,0,0,0,0,0,0,0,0]^T$ and $\mathbf{Y}_i(\xi) = [N_i(\xi), Q_{2i}(\xi), Q_{3i}(\xi), M_{1i}(\xi), M_{2i}(\xi), M_{3i}(\xi), u_i(\xi), \phi_i(\xi), v_i(\xi), \frac{\mathrm{d}v_i(\xi)}{\mathrm{d}\xi}, w_i(\xi), \frac{\mathrm{d}w_i(\xi)}{\mathrm{d}\xi}]^T$.

$$\mathbf{A}_i^{11} = \begin{bmatrix} 0 & 0 & \frac{-1}{R_i} & 0 & 0 & 0 \\ 0 & 0 & 0 & 0 & 0 & 0 \\ \frac{1}{R_i} & 0 & 0 & 0 & 0 & 0 \\ 0 & 0 & 0 & 0 & 0 & \frac{-1}{R_i} \\ 0 & 0 & 1 & 0 & 0 & 0 \\ 0 & -1 & 0 & \frac{1}{R_i} & 0 & 0 \end{bmatrix}, \tag{13}$$

$$\mathbf{A}_i^{21} = \begin{bmatrix} \frac{1}{EF} & 0 & 0 & 0 & 0 & 0 \\ 0 & 0 & 0 & \frac{1}{K} & 0 & 0 \\ 0 & 0 & 0 & 0 & 0 & 0 \\ 0 & 0 & 0 & 0 & 0 & \frac{1}{EJ_3} \\ 0 & 0 & 0 & 0 & 0 & 0 \\ \frac{2}{EFR_i} & 0 & 0 & 0 & \frac{-1}{EJ_2} & 0 \end{bmatrix}, \tag{14}$$

$$\mathbf{A}_i^{22} = \begin{bmatrix} 0 & 0 & 0 & 0 & \frac{-1}{R_i} & 0 \\ 0 & 0 & 0 & \frac{-1}{R_i} & 0 & 0 \\ 0 & 0 & 0 & 1 & 0 & 0 \\ 0 & \frac{1}{R_i} & 0 & 0 & 0 & 0 \\ 0 & 0 & 0 & 0 & 0 & 1 \\ 0 & 0 & 0 & 0 & \frac{-1}{R_i^2} & 0 \end{bmatrix} \tag{15}$$

and $\mathbf{A}_i^{12} = \mathbf{0}_{6\times 6}$, E is the equivalent Young's modulus of the superconducting coil, $K = G\kappa$ is the torsional rigidity of the section about the ξ-axis, G is the equivalent shear elastic constant. The equivalent elastic constants, E and G, can be determined by the theory of composite materials (Miya et al., 1980; Miya and Uesaka, 1982); κ is given by (Timoshenko and Goodier, 1970):

$$\kappa = \frac{b^3 h}{3} - \frac{64b^4}{\pi^5} \sum_{m=1,3,5,\ldots}^{\infty} \frac{1}{m^5} \tanh \frac{m\pi h}{2b} \tag{16}$$

where b and h are the width and height of the rectangular cross-section of the coil, respectively. Moreover, the continuity conditions $\mathbf{Y}(\xi_{ie}) = \mathbf{Y}(\xi_{(i+1)b})$ should be also satisfied. Here, 'ie' means the end of i-th arc, and '$(i+1)b$' means the beginning of $(i+1)$-th arc. When the coil is clamped, we have the boundary conditions as follows:

$$\xi = \xi_{1b}, \text{ and } \xi = \xi_{Ne}: \quad \mathbf{U} = \mathbf{0}, \quad \phi = 0, \quad \frac{\mathrm{d}v}{\mathrm{d}\xi} = 0, \quad \frac{\mathrm{d}w}{\mathrm{d}\xi} = 0. \tag{17}$$

Thus, the solution to Eqs. (1)–(6) can be obtained by solving N sets of Eq. (12) with one set of boundary conditions, that is, Eq. (17) and $N-1$ sets of continuity conditions.

Here, we first solve the homogeneous equation of Eq. (12) for the i-th arc. The general solution, $\mathbf{Y}_{gi}(\xi)$, of Eq. (12) for $\mathbf{F}_i(\xi) \equiv \mathbf{0}$ can be expressed as:

$$\mathbf{Y}_{gi}(\xi) = \mathbf{G}_i(\xi)\mathbf{C}_i, \tag{18}$$

where $\mathbf{C}_i = [\mathrm{C}_{i1}, \mathrm{C}_{i2}, \ldots, \mathrm{C}_{i12}]^T$ is an unknown constant matrix; $\mathbf{G}_i(\xi)$ is a closed fundamental solution matrix composed of four submatrixes $\mathbf{G}_i^{kl}(\xi)$ $(k,l = 1,2)$, that is, $\mathbf{G}_i^{12}(\xi) = \mathbf{0}_{6\times 6}$,

$$\mathbf{G}_i^{11}(\xi)=\begin{bmatrix} 0 & \sin\frac{\xi}{R_i} & \cos\frac{\xi}{R_i} & 0 & 0 & 0 \\ 1 & 0 & 0 & 0 & 0 & 0 \\ 0 & -\cos\frac{\xi}{R_i} & \sin\frac{\xi}{R_i} & 0 & 0 & 0 \\ R_i & 0 & 0 & 0 & \sin\frac{\xi}{R_i} & \cos\frac{\xi}{R_i} \\ 0 & -R_i\sin\frac{\xi}{R_i} & -R_i\cos\frac{\xi}{R_i} & 1 & 0 & 0 \\ 0 & 0 & 0 & 0 & -\cos\frac{\xi}{R_i} & \sin\frac{\xi}{R_i} \end{bmatrix}, \tag{19}$$

$$\mathbf{G}_i^{21}(\xi)=\begin{bmatrix} 0 & t_{1d}+t_1\cos\frac{\xi}{R_i} & t_{1c}-t_1\sin\frac{\xi}{R_i} & \frac{R_i\xi}{EJ_2} & 0 & 0 \\ 0 & 0 & 0 & 0 & t_{2d}-t_2\cos\frac{\xi}{R_i} & t_{2c}+t_2\sin\frac{\xi}{R_i} \\ \frac{R_i^2\xi}{K} & 0 & 0 & 0 & -R_it_{2d}-\frac{R_i^2}{\xi}t_{2c} & \frac{R_i^2t_{2d}}{\xi}-R_it_{2c} \\ \frac{R_i^2}{K} & 0 & 0 & 0 & -t_{2c} & t_{2d} \\ 0 & -t_{1c} & t_{1d} & -\frac{R_i^2}{EJ_2} & 0 & 0 \\ 0 & \frac{-t_{1c}}{\xi}+\frac{t_{1d}}{R_i} & \frac{t_{1c}}{R_i}+\frac{t_{1d}}{\xi} & 0 & 0 & 0 \end{bmatrix}, \tag{20}$$

$$\mathbf{G}_i^{22}(\xi)=\begin{bmatrix} 1 & \cos\frac{\xi}{R_i} & -\sin\frac{\xi}{R_i} & 0 & 0 & 0 \\ 0 & 0 & 0 & 0 & \cos\frac{\xi}{R_i} & -\sin\frac{\xi}{R_i} \\ 0 & 0 & 0 & 1 & -R_i\cos\frac{\xi}{R_i} & R_i\sin\frac{\xi}{R_i} \\ 0 & 0 & 0 & 0 & \sin\frac{\xi}{R_i} & \cos\frac{\xi}{R_i} \\ 0 & \sin\frac{\xi}{R_i} & \cos\frac{\xi}{R_i} & 0 & 0 & 0 \\ 0 & \frac{1}{R_i}\cos\frac{\xi}{R_i} & -\frac{1}{R_i}\sin\frac{\xi}{R_i} & 0 & 0 & 0 \end{bmatrix}, \tag{21}$$

in which

$$D_1=\frac{2}{EFR_i}+\frac{R_i}{EJ_2},\quad D_2=\frac{1}{ER_iJ_3}+\frac{1}{KR_i}, \tag{22}$$

$$t_1 = \frac{D_1 R_i^2}{2} - \frac{R_i}{EF}, \quad t_2 = \frac{D_2 R_i^2}{2} - \frac{R_i}{EJ_3}, \tag{23}$$

$$t_{1d} = \frac{D_1 R_i \xi}{2} \sin\frac{\xi}{R_i}, \quad t_{1c} = \frac{D_1 R_i \xi}{2} \cos\frac{\xi}{R_i}, \tag{24}$$

$$t_{2d} = \frac{D_2 R_i \xi}{2} \sin\frac{\xi}{R_i}, \quad t_{2c} = \frac{D_2 R_i \xi}{2} \cos\frac{\xi}{R_i}. \tag{25}$$

Secondly, we will obtain the particular solution $\mathbf{Y}_{pi}(\xi)$ to Eq. (12) for the applied load $\mathbf{F}_i(\xi)$ by using the finite difference method. Let us divide the i-th arc $[\xi_{ib},\xi_{ie}]$ into M elements, such that

$$\xi_{ib} = \xi_{i0} < \xi_{i1} < \xi_{i2} < \ldots < \xi_{i(M-1)} < \xi_{iM} = \xi_{ie}. \tag{26}$$

Denoting $\mathbf{Y}_{pi}^{j} = \mathbf{Y}_{pi}(\xi)|_{\xi=\xi_j}$ ($j = 0,1,2,\ldots, M$), we have

$$\mathbf{Y}_{pi}^{j+1} = \mathbf{Y}_{pi}^{j} + \left[\mathbf{A}_i \mathbf{Y}_{pi}^{j} + \mathbf{F}_i(\xi_j)\right] \Delta\xi_j, \tag{27}$$

in which $\delta\xi_j = \xi_{j+1} - \xi_j$. Since a particular solution is independent of the boundary conditions, it is obvious that the particular solution $\mathbf{Y}_{pi}(\xi)$ can be iteratively obtained once the initial value of the iteration $\mathbf{Y}_{pi}(\xi_{ib})$ is given arbitrarily.

After the general solution given by Eq. (18) and the particular solution given by Eq. (27) are obtained, we can write the solution to Eq. (12) for a pre-given magnetic force as follows:

$$\mathbf{Y}_i(\xi) = \mathbf{Y}_{gi}(\xi) + \mathbf{Y}_{pi}(\xi) = \mathbf{G}_i(\xi)\mathbf{C}_i + \mathbf{Y}_{pi}(\xi). \tag{28}$$

Denoting $\mathbf{Y}_{gi}(\xi_{ib}) = \mathbf{Y}_{gi}(\xi)|_{\xi=\xi_{ib}}$ and $\mathbf{Y}_{pi}(\xi_{ib}) = \mathbf{Y}_{pi}(\xi)|_{\xi=\xi_{ib}}$, respectively, we can finally express the unknown constant matrix $\mathbf{C}_i$ in the form

$$\mathbf{C}_i = [\mathbf{G}_i(\xi_{ib})]^{-1}[\mathbf{Y}_i(\xi_{ib}) - \mathbf{Y}_{pi}(\xi_{ib})]. \tag{29}$$

Further,

$$\mathbf{Y}_i(\xi) = \mathbf{G}_i(\xi)[\mathbf{G}_i(\xi_{ib})]^{-1}[\mathbf{Y}_i(\xi_{ib}) - \mathbf{Y}_{pi}(\xi_{ib})] + \mathbf{Y}_{pi}(\xi). \tag{30}$$

The above expression can also be written as follows:

$$\begin{aligned}\mathbf{Y}_i(\xi) = {} & \mathbf{G}_i(\xi)[\mathbf{G}_i(\xi_{ib})]^{-1} \cdot \mathbf{T}_{i-1} \cdot \mathbf{T}_{i-2} \ldots \mathbf{T}_1 \cdot [\mathbf{Y}_1(\xi_{1b}) - \mathbf{Y}_{p1}(\xi_{1b})] + \mathbf{Y}_{pi}(\xi) + \mathbf{G}_i(\xi)[\mathbf{G}_i(\xi_{ib})]^{-1} \\ & \cdot \Big\{[\mathbf{Y}_{p(i-1)}(\xi_{(i-1)e}) - \mathbf{Y}_{pi}(\xi_{ib})] + \mathbf{T}_{i-1} \cdot [\mathbf{Y}_{p(i-2)}(\xi_{(i-2)e}) - \mathbf{Y}_{p(i-1)}(\xi_{(i-1)b})] + \mathbf{T}_{i-1} \cdot \mathbf{T}_{i-2} \\ & \cdot [\mathbf{Y}_{p(i-3)}(\xi_{(i-3)e}) - \mathbf{Y}_{p(i-2)}(\xi_{(i-2)b})] + \ldots + \mathbf{T}_{i-1} \cdot \mathbf{T}_{i-2} \ldots \mathbf{T}_2 \cdot [\mathbf{Y}_{p1}(\xi_{1e}) - \mathbf{Y}_{p2}(\xi_{2b})]\Big\}.\end{aligned} \tag{31}$$

In order to simplify the solving programe, we choose the particular solution which satisfies the continuity condition $\mathbf{Y}_{pi}(\xi_{ib}) = \mathbf{Y}_{p(i-1)}(\xi_{(i-1)e})$, Eq. (31) is then

$$\mathbf{Y}_i(\xi) = \mathbf{G}_i(\xi)[\mathbf{G}_i(\xi_{ib})]^{-1} \cdot \mathbf{T}_{i-1} \cdot \mathbf{T}_{i-2} \ldots \mathbf{T}_1 \cdot [\mathbf{Y}_1(\xi_{1b}) - \mathbf{Y}_{p1}(\xi_{1b})] + \mathbf{Y}_{pi}(\xi), \tag{32}$$

in which $\mathbf{T}_i = \mathbf{G}_i(\xi_{ie})[\mathbf{G}_i(\xi_{ib})]^{-1}$, and the unknown, $\mathbf{Y}_1(\xi_{1b})$, can be determined by the boundary conditions at $\xi = \xi_{1b}$ and $\xi = \xi_{Ne}$, i.e., Eq. (17).

It should be noted here that Eq. (32) is obtained for the case when the applied magnetic force is known *a priori*. However, since the magnetic force acting on the coil c depends on its deformation, the force is not known until the deformation is determined. In order to solve this kind of nonlinear coupling problem between the magnetic force and the deformation of the coil c, we need to calculate the magnetic force $\mathbf{q} = \mathbf{q}_n$ by Eq. (7) for a pre-given displacement $\mathbf{U} = \mathbf{U}_n$. Then, we get a new displacement $\mathbf{U} = \mathbf{U}_{n+1}$ of the coil c under the magnetic force $\mathbf{q}_n$ from Eq. (32). This iteration procedure will be repeated until the condition

$$\|\mathbf{U}_{n+1} - \mathbf{U}_n\| < \delta \tag{33}$$

is satisfied. Here, $0 < \delta \ll 1$ is a prescribed tolerance, and n denotes the number of iteration.

4. Numerical results

Here, we focus our attention on the magnetoelastic bending and snapping of the non-circular coil c in a three-coil superconducting partial torus. The material and geometrical parameters of the coil c adopted by the numerical examples are as follows: $E = 2.7 \times 10^{10}$ pa, $G = 3.4 \times 10^{9}$ pa, $\theta_r = \theta_l = 22.5^\circ$, $h = 0.6$ mm, $a = 50$ mm, $b = 9$ mm and $c = 40$ mm, which are the same ones as Miya and Uesaka (1982) used in their experiments. In order to confirm the validity of our theoretical analysis and calculation code, we compare the theoretical prediction of critical snapping current with the experimental data for a circular coil. Our numerical result is 48.09 A/turn, which is much closer to Miya

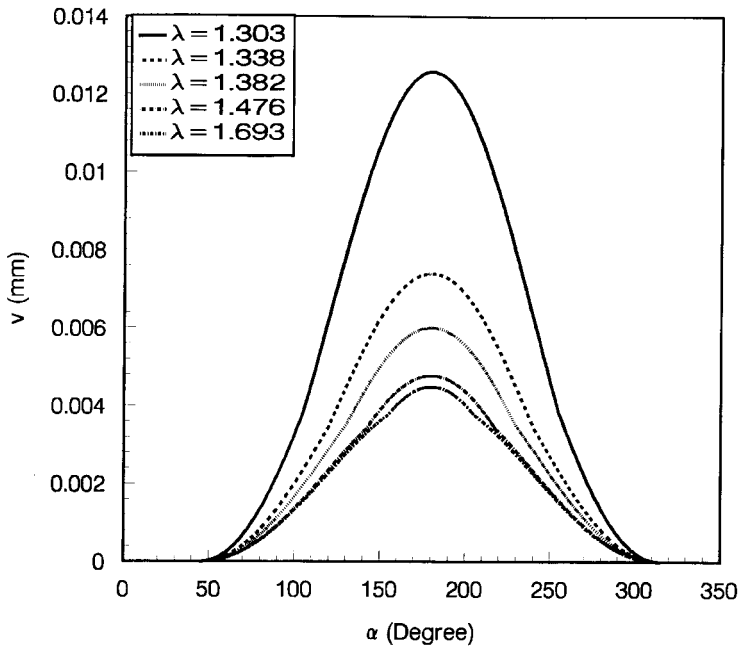

Fig. 2. Out-of-plane transverse deflection distribution for non-circular coil ($I = 74.5$ A/turn).

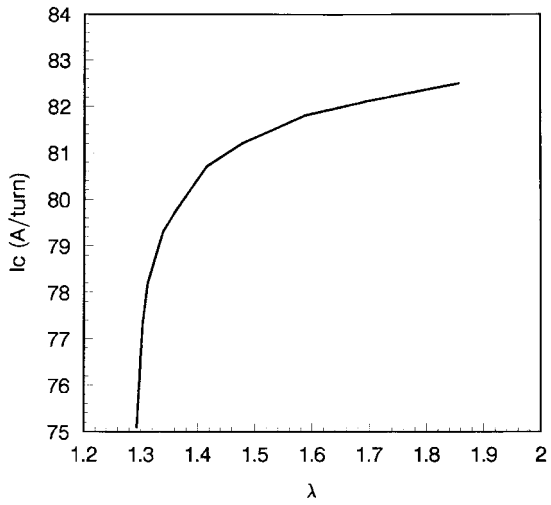

Fig. 3. Critical current value vs. radius ratio $\lambda = R_1/R_2$.

et al.'s experimental data, 47.8 A/turn. So, we can conclude that our theoretical model and numerical program are reliable and reasonable.

For a non-circular coil composed of three circular arcs as shown in Fig. 1, the distributions of the displacement and the internal force components are obtained by the theoretical model and the semi-analytical method presented in this paper and shown in Figs. 2, 4 and 5. Due to the symmetry in both the geometry and the magnetic field of the coil c about the horizontal axis (i.e. the y–O–z plane), the distributions of the displacement and the internal force exhibit the symmetry property as expected. It is found in Fig. 2 that the transverse displacement of the coil is much larger than the in-plane one.

The effects of radius ratio $\lambda = R_1/R_2$ on the distributions of the displacement, the internal force and the the critical snapping current are quantitatively discussed. Fig. 2 shows that the transverse displacement v decreases with the increase of the radius ratio $\lambda = R_1/R_2$. The critical snapping current vs. radius ratio $\lambda = R_1/R_2$ is plotted in Fig. 3. It is obvious that the critical snapping current increases with $\lambda = R_1/R_2$, and the increment of the critical snapping current for $\lambda = R_1/R_2 < 1.382$ is faster than that for $\lambda = R_1/R_2 > 1.382$. From Fig. 4, we find that the in-plane displacement components u and w decrease with the increase of radius ratio $\lambda = R_1/R_2$ when $1 < \lambda < 1.382$, and increase when $\lambda > 1.382$. When λ is near about 1.382, the displacements, u and w, are almost the minimum ones. The distributions of the internal force components N and M_2 are shown in Fig. 5. Aside from their maximum values, taken place at the two ends of the coil, decrease with the increase of $\lambda = R_1/R_2$, the fluctuation of the internal force near the middle region of the coil is within a narrow range when $\lambda = R_1/R_2$ is near 1.382.

The effect of a unsymmetrical alignment on the critical snapping current for a circular coil is also discussed. The assymmetry is described by a small inclination angle, α_0 (see Fig. 1). The maximum transverse deflection of the circular coil versus the carrying current for a given angle α_0 is shown in Fig. 6. From Fig. 6, one can find that there exists a bending deformation for the coil before the snapping happens. The larger the angle, the more obviously the bending deformation. The critical snapping current versus the inclination angle α_0 are shown in Fig. 7. The inclination angle, α_0, lowers the critical snapping current. Therefore, the theoretical values of the critical snapping current for the coils placed symmetrically should be higher than the experimental ones, since some small misalignments are unavoidable in practice.

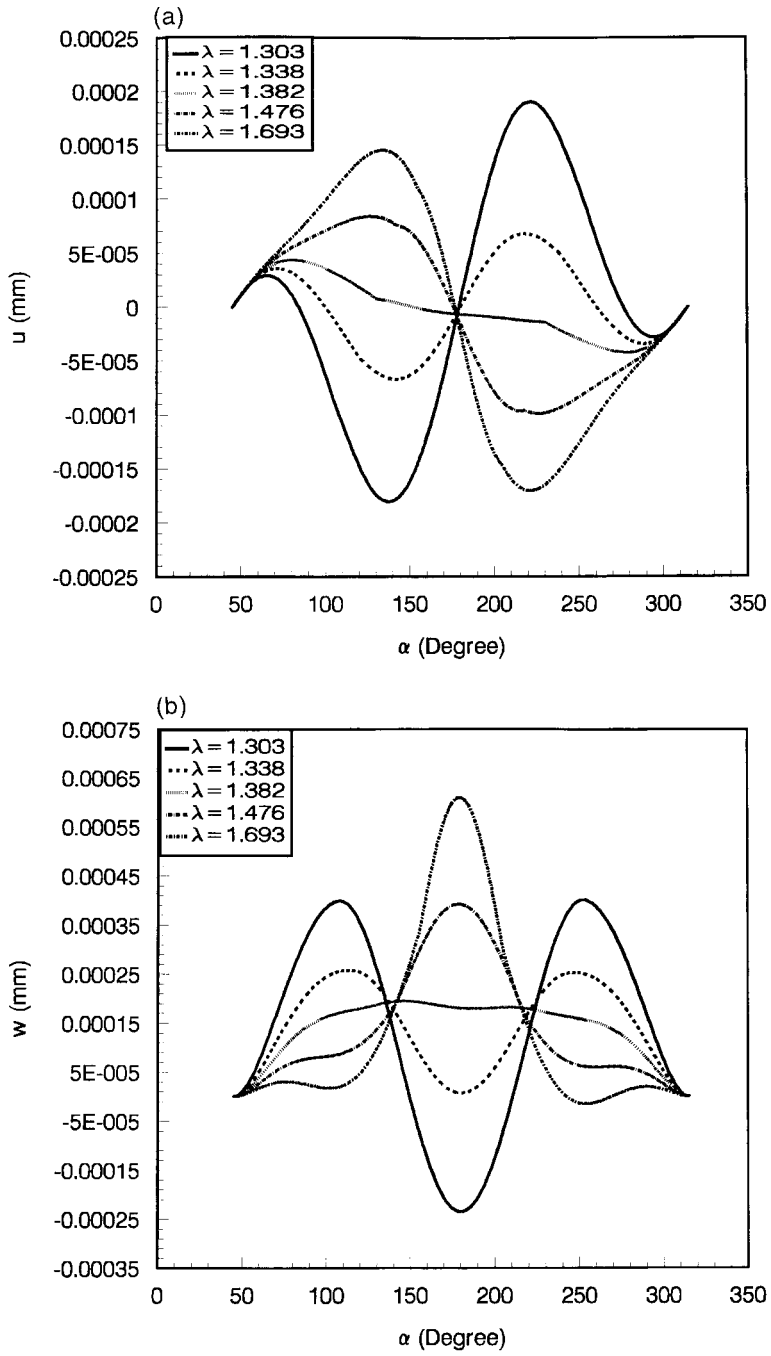

Fig. 4. In-plane displacement distribution for non-circular coil (I = 74.5 A/turn): (a) displacement u, (b) displacement w.

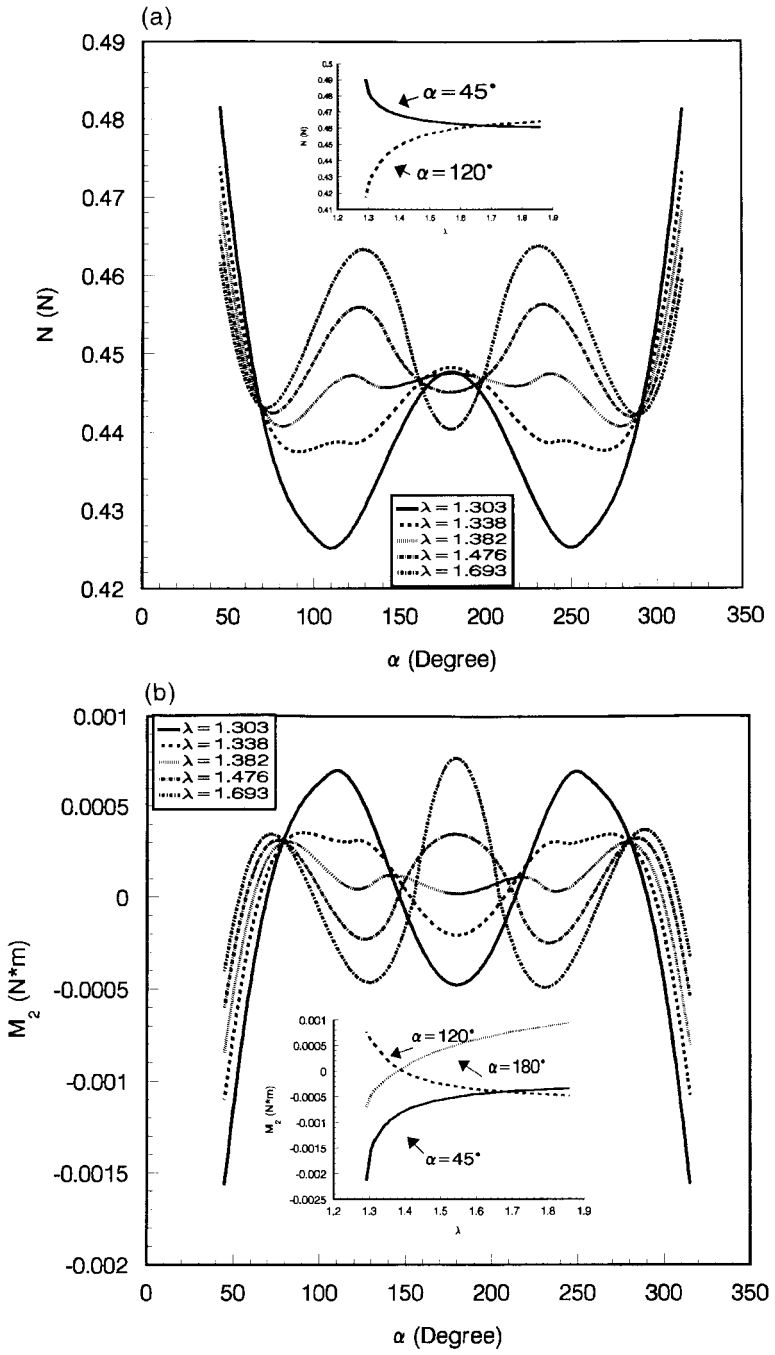

Fig. 5. Internal force distribution for non-circular coil (I = 74.5 A/turn): (a) extension force N, (b) bending moment M_2.

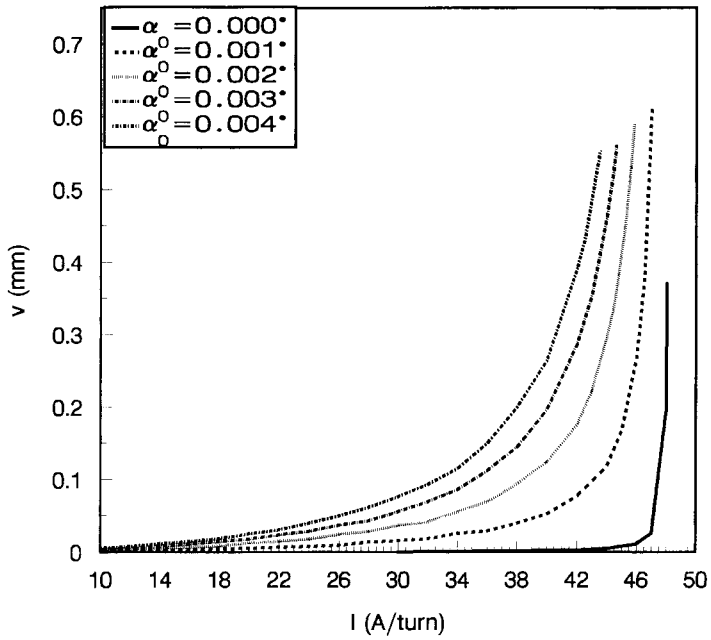

Fig. 6. Maximum transverse deflection vs. carrying current ($R_1 = R_2 = 64.5$ mm).

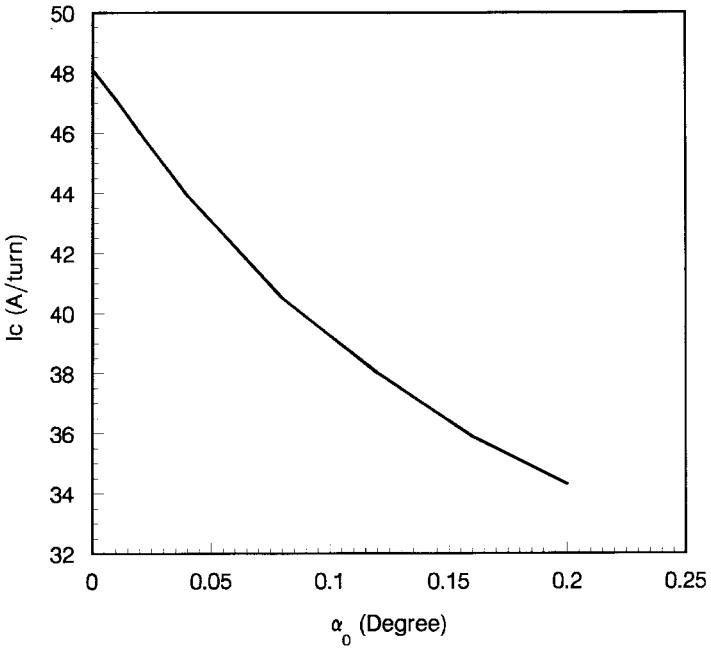

Fig. 7. Critical current vs. disturbance angle α_0 ($R_1 = R_2 = 64.5$ mm).

5. Conclusions

With the aid of the Biot–Savart law and the curved beam theory, a theoretical analysis for magnetoelastic bending and snapping of the current-carrying non-circular coil is presented in this paper. The mechanical behavior of the coil in the partial torus is simulated by a semi-analytical solving method. The numerical results show that the non-circular coil has a much better stability than the circular one since the values of the critical snapping current are distinctly heightened with the increase of ratio $\lambda = R_1/R_2$. The distributions of the displacement and the internal force fluctuate in a narrow range when $\lambda = R_1/R_2$ is near about 1.382, which means that there possibly exists an optimum mechanical state for a non-circular coil when the radius ratio $\lambda = R_1/R_2$ is near 1.382. The numerical results also confirm that the initial inclination angle arising from the misalignments of the coils makes the critical snapping current lower. These results are useful in the design of a fusion reactor.

Acknowledgements

Supported by the NSFC Outstanding Youth Science Foundation (19725207) and the NECC Outstanding Young Teacher Foundation.

References

Geiger, W., Jungst, K.P., 1991. Buckling calculations and measurements on a technologically relevant toroidal magnet system. ASME J. Appl. Mech. 58, 167–174.

Love, A.E.H., 1944. The Mathematical Theory of Elasticity. Dover, New York.

Miya, K., Takagi, T., Uesaka, M., 1980. Finite element analysis of magnetoelastic buckling and experiments on a three-coil superconducting partial torus. In: Moon, F.C. (Ed.), Mechanics of Superconducting Structures. ASME, New York, pp. 91–107.

Miya, K., Uesaka, M., 1982. An application of finite element method to magnetomechanics of superconducting magnets for magnetic reactors. Nuclear Engineering and Design 72, 275–296.

Moon, F.C., 1976. Buckling of a superconducting coil nested in a three-coil toroidal segment. J. Appl. Phys. 47, 920–921.

Moon, F.C., 1984. Magneto–Solid Mechanics. John Wiley and Sons, New York.

Moon, F.C., Swanson, C., 1977. Experiments on buckling and vibration of superconducting coils. ASME J. Appl. Mech. 44, 707–713.

Motojima, O., 1993. LHD magnet system design and construction. In: ANS 11th Topical Meeting of the Thechnology of Fusion Energy June 19–23 1994, New Orleans, USA.

Timoshenko, S.P., Goodier, J.N., 1970. Theory of Elasticity, 3rd ed. McGraw–Hill Book Co.

Zhou, Y.H., Zheng, X.J., Miya, K., 1995. Magnetoelastic bending and buckling of three-coil superconducting partial torus. Fusion Engineering and Design 30, 275–289.